24th COBEM - 2017

24th ABCM International Congress of Mechanical Engineering
December 3-8, 2017, Curitiba, PR, Brazil

COBEM-2017-0430
STUDY OF SCALE-ADAPTIVE SIMULATION MODEL IN RECIRCULATING FLOWS.

Luiz Otavio de Carvalho Bovolato
Paulo Celso Greco Junior
University of São Paulo, Department of Aeronautical Engineering, 13563-120, São Carlos, SP, Brazil
e-mails: luiz.bovolato@usp.br, pgreco@sc.usp.br

Abstract. *The project proposed aims to evaluate the capability of the Scale-Adaptive Simulation (SAS) model in order to predict mean flow characteristics and important turbulent structures of recirculating flows present in gas turbine combustors. In that case, two benchmark cases were selected, whose flow characteristics have similar behavior to some combustor flow portions: (i) Backward-Facing Step Flow; (ii) Flow through a swirler model. Comparisons were made between Reynolds Averaged Navier-Stokes (RANS), Large-Eddy Simulation (LES), SAS and empirical/numerical results. Numerical analyses were performed using the software Ansys CFX. As can be noted in the Backward-Facing Step case, the SAS model presents a good correlation with experimental results only inside the recirculation zone and, therefore, a better understanding of its numerical mechanisms is needed. For the swirler study case, SAS presents close results to experimental data for regions far from swirler outlet so that a longer simulation time is desirable.*

Keywords: *Scale-Adaptive Simulation, Large-Eddy Simulation, Reynolds Averaged Navier-Stokes, Backward-Facing Step Flows, Swirl Flows.*

1. INTRODUCTION

Environment requirements, increasingly rigorous, have being employed to regulate combustion engineering design devices due to several environmental effects related to global warming. Thus, a growing need to use computational tools, such as computational fluid dynamics, has become necessary in order to create optimized designs. For the design of gas turbine combustors, a satisfactory characterization of non-reactive flow behavior is desirable because it has a great influence on the combustion efficiency as, e. g., regions presenting recirculating flows, which ones will be discussed in the present study.

Currently, the Large Eddy Simulation (LES) model has been used for combustion chamber flow analysis. However, LES demands a high computational cost compared to the Reynolds Averaged Navier-Stokes (RANS) method, as described by Michelassi, *et al*., 2003, so that it is unfeasible to be employed at high Reynolds number flow studies. Thus, the use of hybrid RANS/LES models, such as Scale-Adaptive Simulation (SAS), seems to be an alternative method in order to overcome possible computational limitations. Other advantages of the SAS model, in relation to the other models, are: a) simpler computational mesh implementation, when compared to mesh implementation for LES, which demands finer grids; b) determination of a broad turbulent frequency spectral content, unlike classic Unsteady Reynolds-Averaged Navier-Stokes (URANS) models.

Thus, in order to validate the SAS model, compared to RANS, LES and experimental data, two case studies were selected, both implemented in ANSYS CFX: Backward-Facing Step Flow and Swirl Flow.

2. COMPUTATIONAL MODELS

2.1 Reynolds Averaged Navier-Stokes

The RANS method consists to decompose equation variables, such as velocity and pressure, into two components: Mean component, $\bar{\phi}$, and Fluctuating component, ϕ',as can be seen in Eq. (1).

$$\phi = \bar{\phi} + \phi' \tag{1}$$

The turbulence model employed in the present work, for RANS analysis, is the Shear Stress Transport (SST), proposed by Menter (1994), which blends k-ω turbulence model (Wilcox, 1986) and k-ε turbulence model (Launder and Spalding, 1974).

2.2 Large-Eddy Simulation

The LES method, firstly suggested by Smagorinsky (1963), consists in applying a spatial filtering at fluid dynamic equation variables as can be seen in Eq. (2), splitting them into a directly solved part and a modeled part:

$$\overline{\emptyset}(x,t) \equiv \frac{1}{V^3} \int_v \emptyset(x',t)\, dx' \tag{2}$$

where V consists in the element control volume. The Germano's dynamics model, proposed by Germano *et al.* (1991), lately modified by Lilly (1992), was used to model subgrid stress tensors. This model consists in proportionality constant, C_s, automatic correction method. Then the subgrid turbulent viscosity is calculated in according to Eq. (3):

$$\mu_{SGS} = \rho (C_s \Delta)^2 |\bar{S}| \tag{3}$$

$$\Delta = V^{1/3} \tag{4}$$

where $|\bar{S}|$ corresponds to the shear stress rate magnitude and Δ corresponds to the filter characteristic lengthscale. The correction is done by applying a double filtering process: the first spatial filtering is done by using the filter characteristic lengthscale; subsequent filtering is done using a larger filter lengthscale. Thus, the proportionality constant is found by using a correlation between both filtering.

2.3 Scale-Adaptive Simulation

Some URANS deficiencies in relation to the turbulence frequency spectra prediction were observed, leading to the development of SAS-SST model (Menter and Egorov, 2010). SAS-SST model adopts practically the same URANS-SST model basic structure. However, it was introduced a source term, Q_{SAS}, in the rate of dissipation equation, as described in Eq. (5). The introduction of the source term enables to the SAS-SST model a LES-like behavior, i. e., a better capability to predict turbulent structures

$$Q_{SAS} = max\left[\rho \zeta_2 k S^2 \left(\frac{L}{L_{vk}}\right)^2 - c \frac{2\rho k}{\sigma_\phi} max\left(\frac{1}{\omega^2}\frac{\partial \omega}{\partial x_j}\frac{\partial \omega}{\partial x_j}, \frac{1}{k^2}\frac{\partial k}{\partial x_j}\frac{\partial k}{\partial x_j}\right), 0\right] \tag{5}$$

where ζ_2, σ_ϕ and c are empirical constants; the variables ω, k, S, L and L_{vk} are, respectively, turbulent frequency, turbulent kinetic energy, shear stress rate magnitude, local characteristic turbulent lengthscale and Von Kárman lengthscale. This latter variable corresponds to a "numerical trigger", in order to solve turbulent structures, as described in Eq. (6):

$$L_{vk} = \kappa S / |\nabla^2 U| \tag{6}$$

where κ is the Von Kárman constant. So, the bigger the local velocity second derivative is in comparison to the local velocity first derivative, or shear stress rate, the greater is the model's capability to predict turbulent structures.

3. CASE STUDIES

3.1. Backward-Facing Step

Next, it is presented an overall description of the backward-facing step flow study case used in this work. This benchmark case was chosen not only due to a simple geometry to be modeled and to be meshed but also due to the recirculating flow structures formed behind the step as a consequence of an abrupt expansion and consequent separation of the flow from the wall. Interesting phenomena, beyond the recirculating structure, occur after flow separation such as mixing layer and free-shear layer. The geometry, flow conditions and empirical results were extracted from Driver and Jovic (1994) work, at which a turbulent flow passing through a channel over a known-height step was analyzed. The Reynolds number based on step height, Re_h, equals to 5000. The geometry and its geometric parameters are illustrated at Fig. (1):

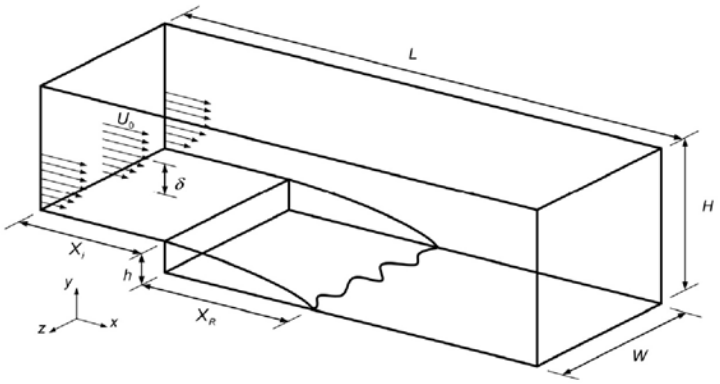

Figure 1. Step domain illustrations of geometrical parameters.

The step is 9.8 milimeters height and the geometric parameters H, W, L e X_i have, respectively, size dimensions correspondent to 6h, 4h, 20h e 3h. The structured meshes generated for SAS and RANS analyses have, approximately, 1.3 million control volume elements and, for LES analysis, it has 6.2 million control volume elements. For both meshes, an in-depth description is shown in Tab.(1):

Table 1. Step domain discretization parameters for RANS, SAS and LES analysis.

	Height (SAS/RANS)	Width (SAS/RANS)	Length (SAS/RANS)	Height (LES)	Width (LES)	Length (LES)
Below Step	45	45	243	75	64	512
Above Step	55	45	280	98	64	592

For inlet boundary condition, it was set a velocity profile extracted from Driver and Jovic (1994). At the domain top, it was chosen a symmetry condition; at domain sides, it was attributed a periodic condition; at the domain bottom, it was set a wall condition and for the outlet boundary condition, it was chosen a relative pressure equals to zero, i. e., outlet absolute pressure equals 1 atm. An isothermal condition for the flow was considered (20^{o}C) and the timesteps chosen for LES and SAS transient analyses considered were $2x10^{-5}$s.

3.2 Swirl Flow

For flow passing through a swirler case study, it was selected the experiment presented in Cai, *et al.*, 2005, from where geometrical parameters and experimental results were taken. In Figure (2) and in Table (2), respectively, the modeled geometry and geometrical parameters are shown.

Table 2. Swirler main geometrical data.

Geometrical Parameters	Size
External Diameter	22,5 mm
Chamber length	304,8 mm
Chamber height/width	50,8 mm

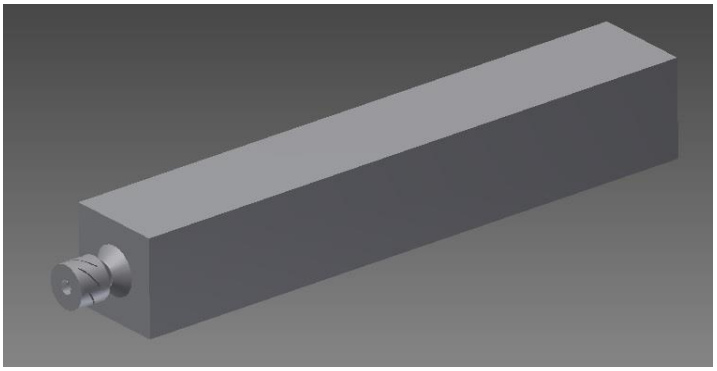

Figure 2. Modeled geometry illustration from geometrical data obtained from Cai, *et al.*, 2005.

The mesh employed in both computational simulations has, approximately, 3.3 million elements. At inlet and outlet boundary conditions, respectively, a mass flow rate equals to 0.49 kg/min and a relative static pressure equals to zero were set. In other geometrical frontiers, a wall condition was applied. The thermal condition was assumed as isothermal flow (21^{o}C) and the timestep considered was 2x10^{-5}s.

4. RESULTS AND DISCUSSION

4.1 Backward-Facing Step

For the backward-facing step case, some RANS, LES and SAS analyses results, in comparison to experimental results and Direct Numerical Simulation data, extracted from Le, *et al.*, 1997, are shown: (i) reattachement length after separation as can be seen in Tab. (3); (ii) mean velocity profiles, in Fig. (4), obtained along vertical line probes, as can be seen in Fig. (3); and (iii) pressure and friction coefficients, respectively described in Eq. (7) and Eq. (8), can be observed in Fig. (4), along a horizontal line probe at the domain bottom and downstream the step, Fig. (3). For SAS and LES analyses, spatial averaging was performed by collecting time-averaged variables at several line probes parallel to those illustrated in Fig. (3) and, then, by computing a mean value along the transversal direction.

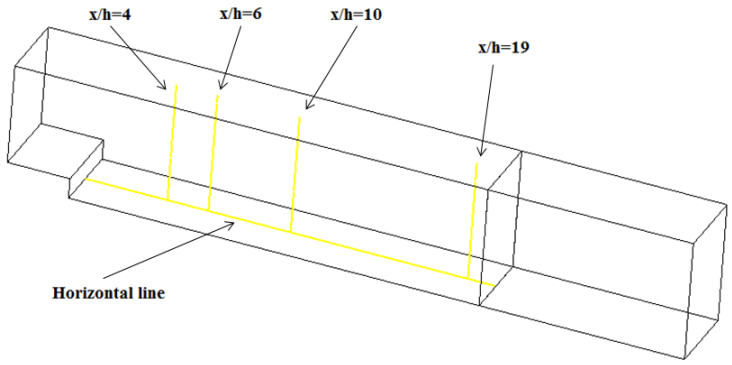

Figure 3. Illustration of vertical and horizontal line probes at backward-facing step domain.

Table 3. Reattachment lengths for different models.

	Reattachment Length (X_r), in function of h
Experimental – Driver e Jovic (1994)	$6 \pm 0{,}15$
RANS	8,09
SAS	8,09
LES	7,74
DNS - Le, Moin e Kim (1997)	6,28

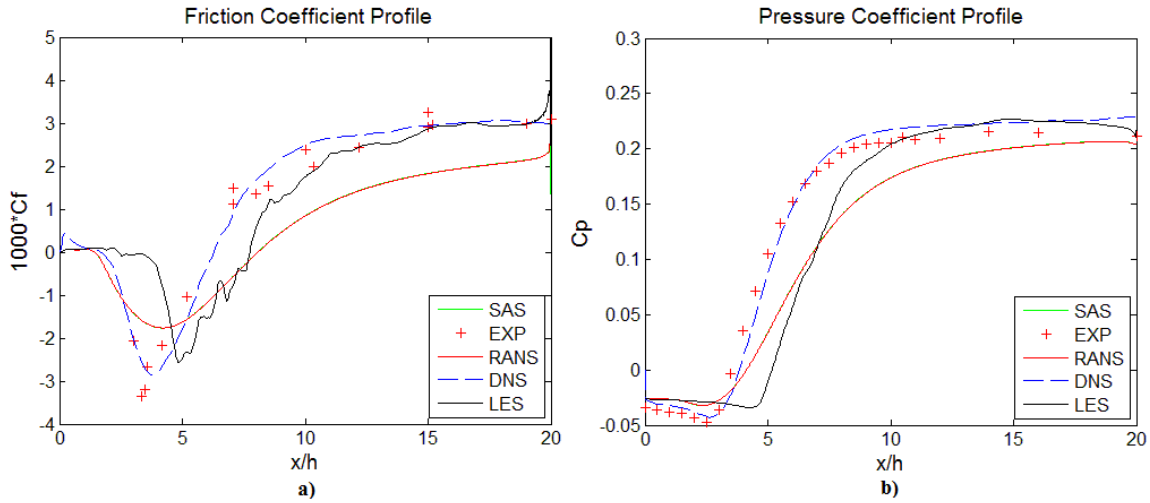

Figure 4. Coefficient profiles along a horizontal line probe a) Friction coefficient profile; b) Pressure coefficient profile.

$$C_p = 2\frac{P-P_{ref}}{\rho U_{ref}} \tag{7}$$

$$C_f = 2\frac{\tau_w}{\rho U_{ref}} \tag{8}$$

where P_{ref}, U_{ref} and τ_w are, respectively, reference pressure, reference velocity and wall shear stress.

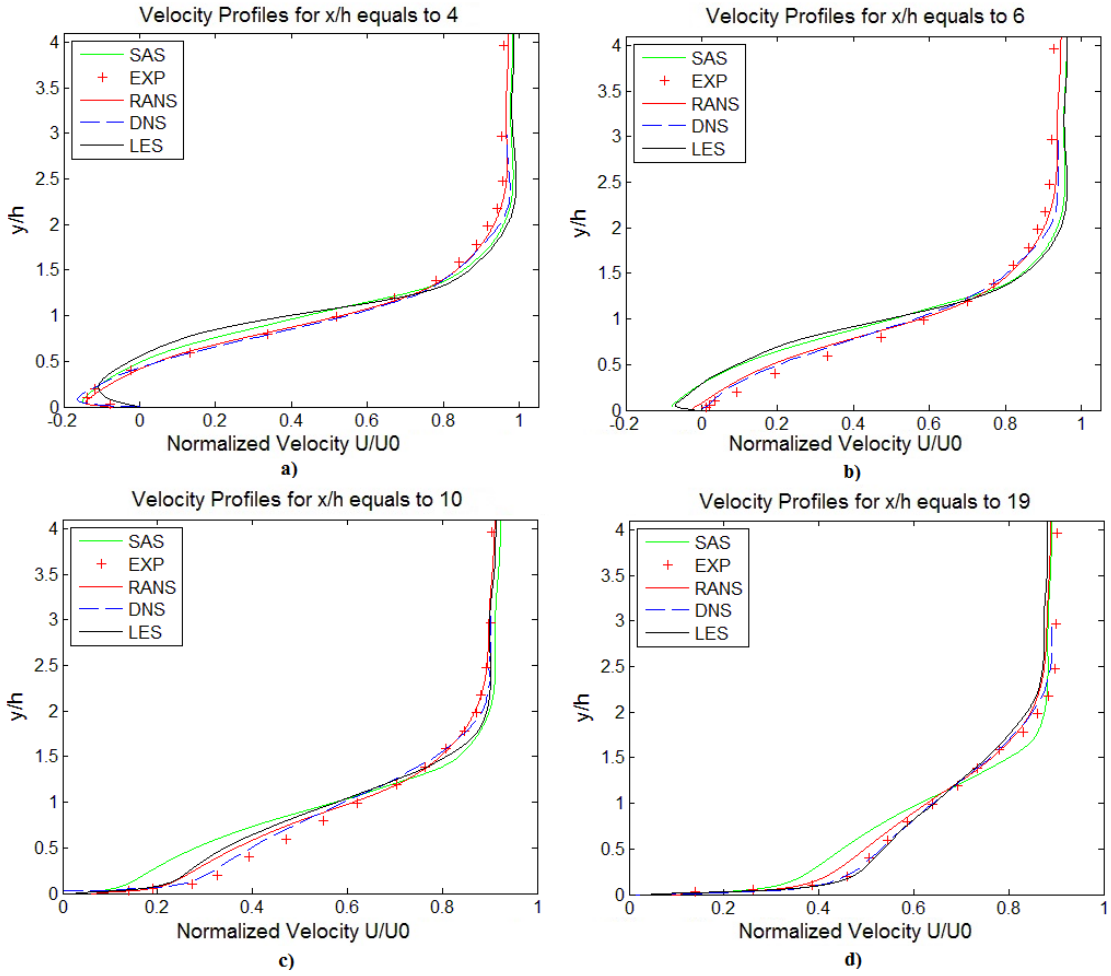

Figure 5. Normalized Velocity profiles far from step at a) 4h; b) 6h; c) 10h; d) 19h.

As can be noted, in Fig. (5), the velocity profiles, obtained at RANS-SST analysis demonstrate a good correlation with experimental results, especially for the ratio y/h greater than one, where the flow behavior does not present effects originated from mixing layer and recirculation flow region. The results obtained at SAS-SST model analysis showed a good agreement with empirical data only for the vertical line probe at x/h equals 4, while, for the other positions, the results obtained presented fair agreement. As discussed by Davidson (2006), in this case, the SAS-SST model may not have presented a distinctive flow behavior, shifting between RANS and LES characteristic behaviors, which may have contributed to a fair correlation. The LES analysis results founded to be very close from experimental ones, except at positions x/h equals 4 and 6. This fact may be explained due to an insufficient sample amount data for better statistical results.

In Figure (4), it is possible to observe that friction and pressure coefficients, downstream the step, showed that RANS-SST and SAS-SST results are coincident, indicating that both models present the same behavior for flows close to walls. However, they did not show a good correlation with experimental and DNS results. LES analysis pressure and friction coefficient results showed better correlations with experimental and DNS data starting from position x/h equals to10, although insufficient sample data is used.

In Table (3), reattachment lengths (X_r) from RANS, SAS and LES model analyses are presented in comparison to experimental and DNS data. As can be noted, LES result presented the best correlation, in comparison to RANS and

SAS model results. These latter models presented a prevailing bi-dimensional flow behavior downstream the step, which characteristic may explain the reattachment delay, as can be seen in Fig. (6):

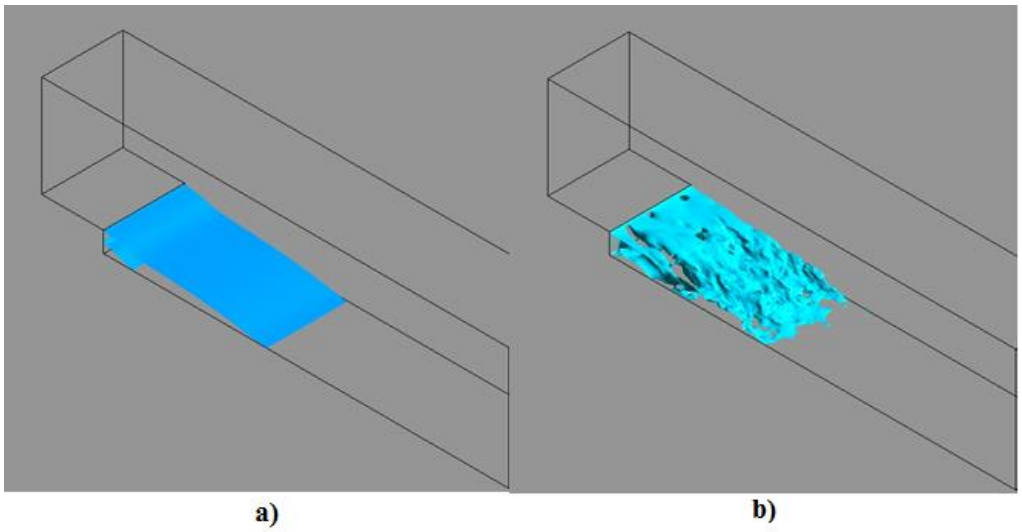

Figure 6. Zero velocity iso-surface downstream the step a) RANS and SAS; b) LES.

4.2 Swirl Flow

For the Swirl flow study case, only URANS-SST and SAS-SST simulations were partially performed until the present moment, however, interesting preliminary conclusions can be drawn. The transient data, took only from 2600 timesteps, were obtained along the transversal direction from six line probes placed at different axial positions, as shown in Fig. (7).

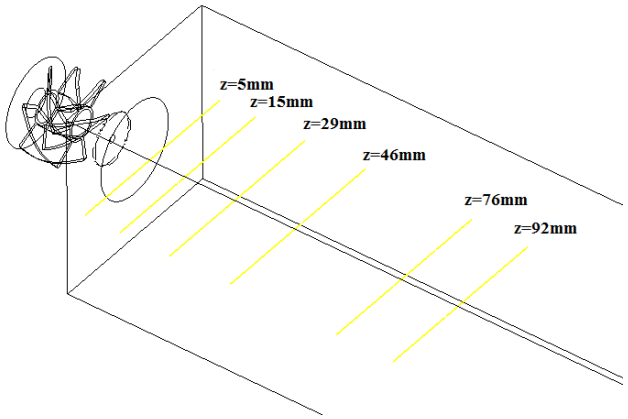

Figure 7. Illustration of horizontal line probes at swirler domain.

Axial, Radial and Tangential time-averaged velocity values, from SAS and URANS simulations, were taken from the transversal probe lines and plotted with experimental data extracted from Cai, *et al.*, 2005, as can be seen from Fig. (8) to Fig. (13).

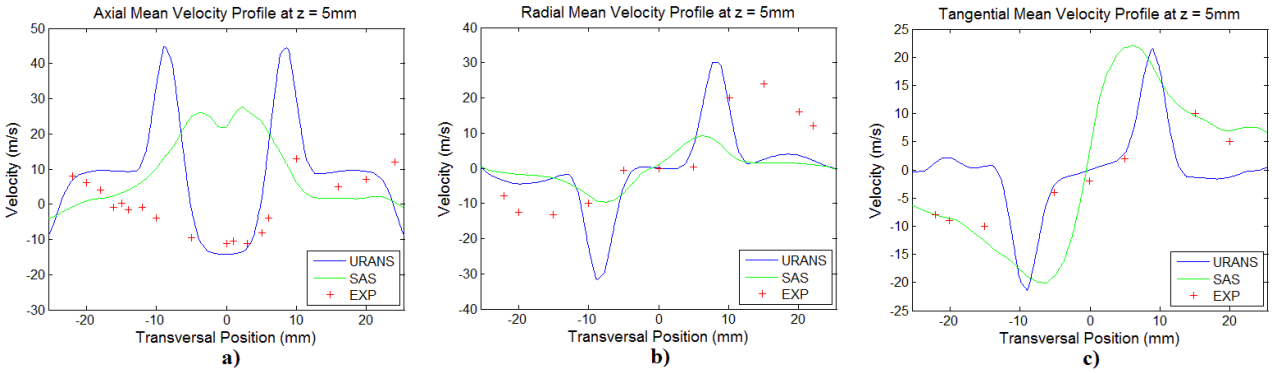

Figure 8. Mean Velocity Profiles for axial position z=5mm a) Axial direction; b) Radial Direction; c) Tangential Direction.

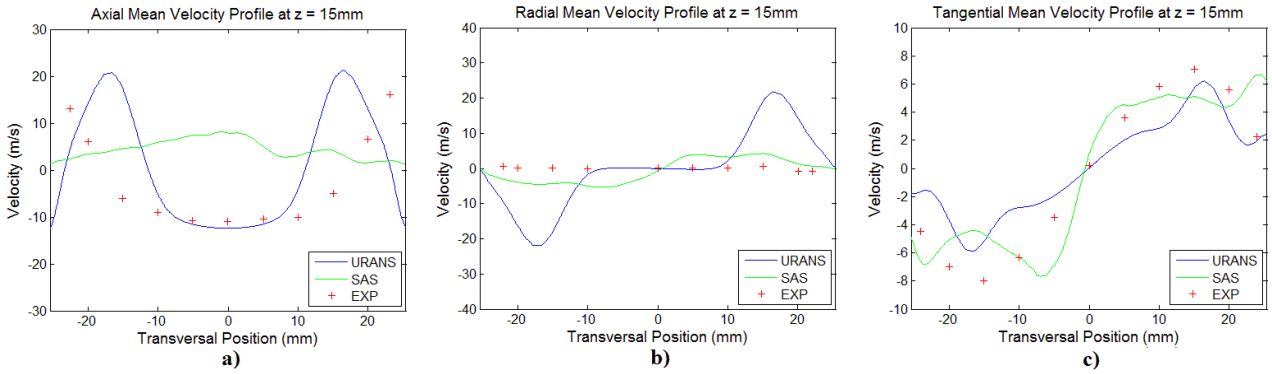

Figure 9. Mean Velocity Profiles for axial position z=15mm a) Axial direction; b) Radial Direction; c) Tangential Direction.

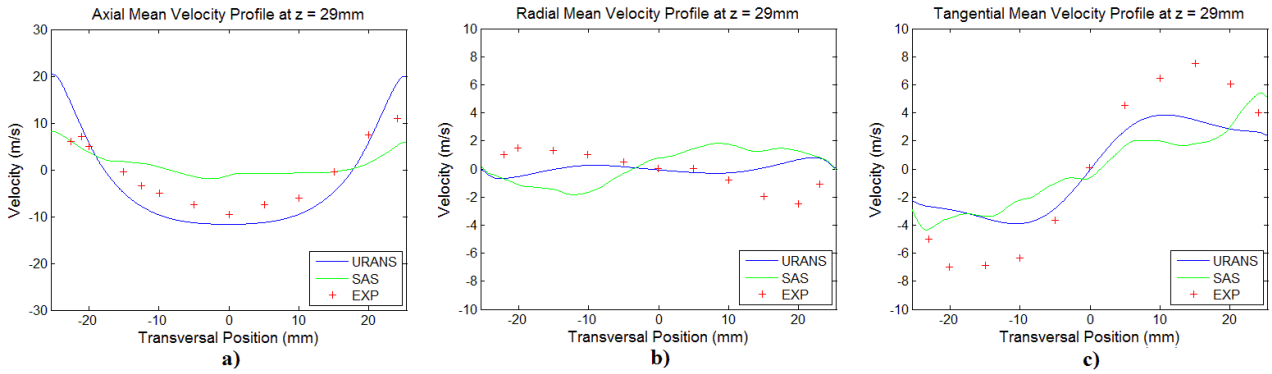

Figure 10. Mean Velocity Profiles for axial position z=29mm a) Axial direction; b) Radial Direction; c) Tangential Direction.

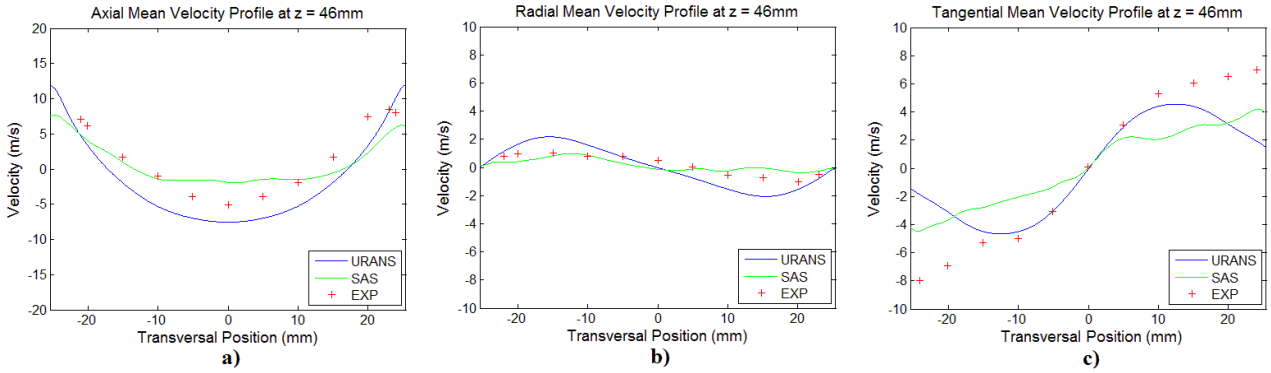

Figure 11. Mean Velocity Profiles for axial position z=46mm a) Axial direction; b) Radial Direction; c) Tangential Direction.

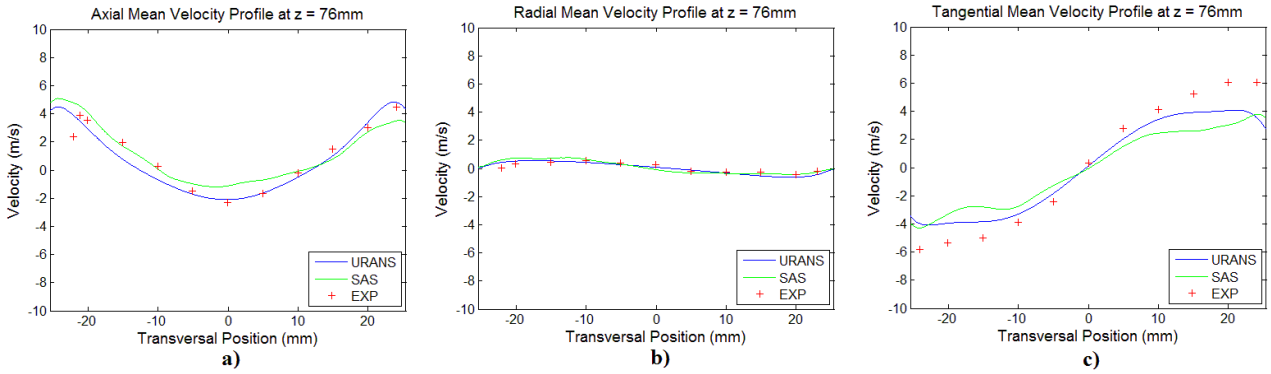

Figure 12. Mean Velocity Profiles for axial position z=76mm a) Axial direction; b) Radial Direction; c) Tangential Direction.

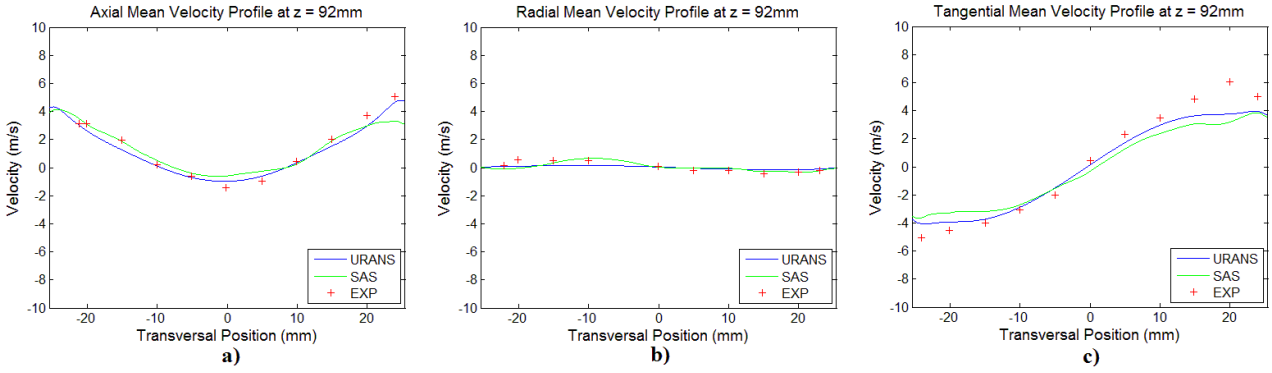

Figure 13. Mean Velocity Profiles for axial position z=92mm a) Axial direction; b) Radial Direction; c) Tangential Direction.

Velocity profile results have shown that, for both models, the presented data have achieved a good correlation with experimental data, except at axial positions z = 5mm and z = 15mm, where mean flow characteristics may not have reached a statistical definitive pattern. In Figure (14), time-averaged velocity streamlines are plotted for both models. Black lines show zero axial speed regions, which ones illustrate the central recirculation zone (CRZ) and corner recirculation zones boundaries. SAS result shows that the CRZ is detached from the channel diffuser outlet, whereas, the CRZ presents at URANS result penetrates into the convergent-divergent channel. Same conclusion can be observed from Fig. (15).

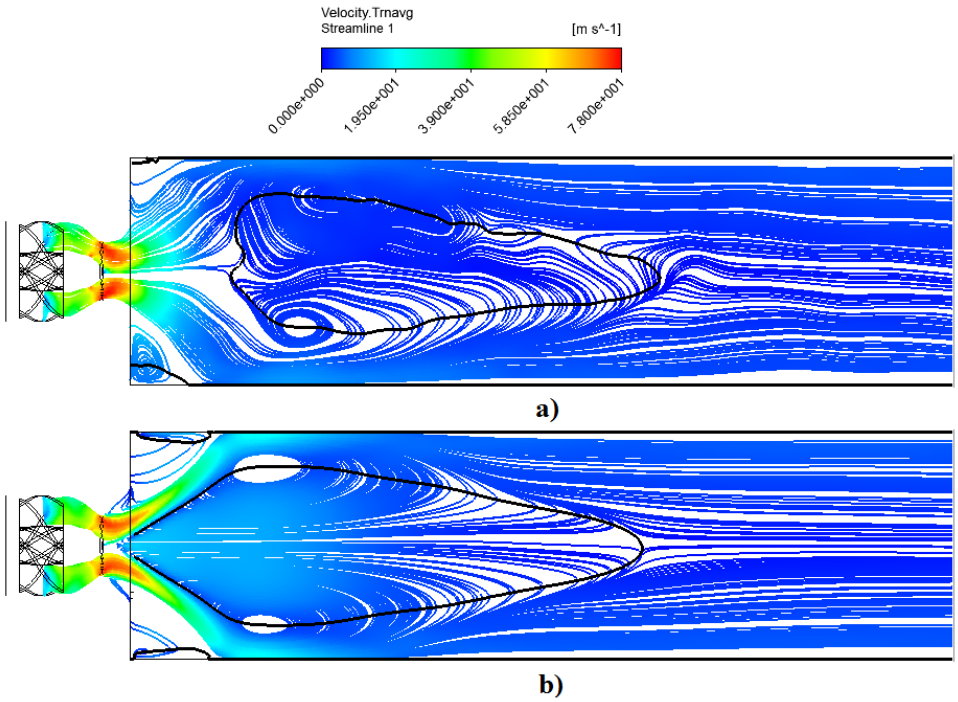

Figure 14. Time-averaged Velocity Streamlines for a) SAS analysis; b) URANS analysis.

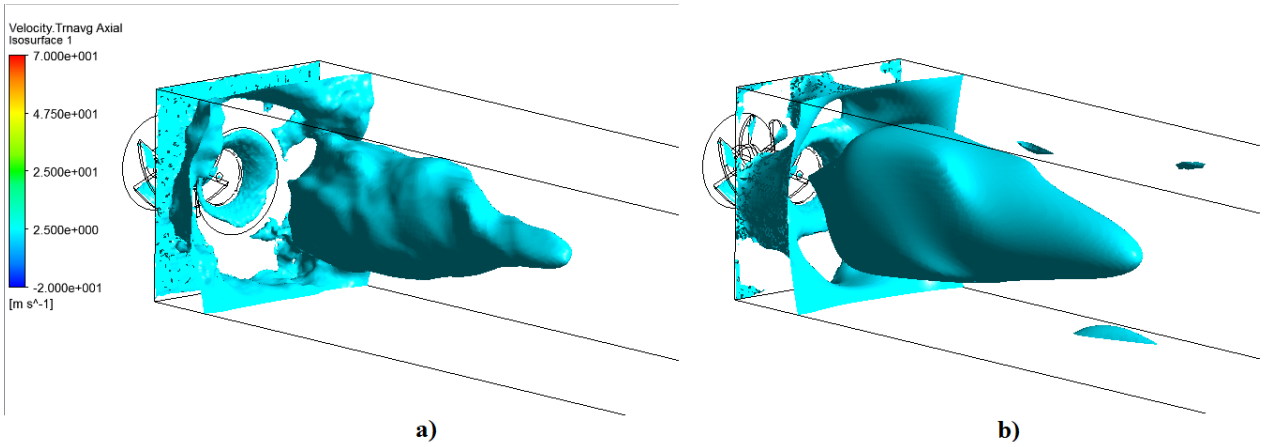

Figure 15. Illustration of iso-surfaces where mean axial velocity equals to zero.

5. CONCLUSIONS

The Scale-Adaptive Simulation had been chosen to be evaluated due to mesh implementation easiness if compared to LES model demanding meshes and due to a better capability to predict flow turbulent spectra if compared to (U)RANS model.

For the backward-facing step study case, the results obtained from SAS model, if compared to RANS model results, demonstrated that the source term, Q_{SAS}, played an important role at velocity profile characteristics. As discussed above, a RANS and LES model behavior mixture may have occurred because no sufficient flow instabilities were introduced so that the SAS model was unable to shift to LES behavior prediction mode. In that case, a better Q_{SAS} trigger process comprehension is necessary. LES model results demonstrated to have good correlation with experimental and DNS results, although it is necessary a greater amount of statistical samples in order to get more accurate results.

For the swirl flow study case, preliminary numerical data from URANS and SAS analyses demonstrated that both model results showed a good correlation in comparison to experimental data in almost probe stations, except for axial positions z=5mm and z=15mm. As can be observed, the central recirculation zone, in both cases, may be out of place as it was expected to be, especially for the SAS analysis, which may be influencing mean velocity profiles at the first

(z=5mm) and second (z=15mm) stations. A longer simulation time will be set, in order to get more accurate and reliable results.

6. ACKNOWLEDGMENTS

The authors are thanked to Sao Carlos Engineering School for all support.

7. REFERENCES

Cai, J., Jeng, S., M., Tacina, R., 2005. "The Structure of a Swirl-Stabilized Reacting Spray Issued from an Axial Swirler." In *43rd AIAA Aerospace Science Meeting and Exhibit, AIAA Paper 2005-1424.* Reno, Nevada.

Davidson, L., 2006. "Evaluation of the SST-SAS model: Channel Flow, Asymmetric Diffuser and Axi-Symmetric Hill." In *European Conference on Computational Fluid Dynamics.* Egmond aan Zee, The Netherlads.

Germano, M., Piomelli, U., Moin, P., Cabot, W. H., 1991. "A Dynamic Subgrid-Scale Eddy Viscosity Model." *Physics of Fluids A, Vol*. 3, p. 1760-1765.

Launder, B. E., Spalding, D. B., 1974. "The numerical computation of turbulent flows." *Computer Methods in Applied Mechanics and Engineering*, Vol. 3, No 2, p. 269-289.

Le, H., Moin, P., Kim, J., 1997. "Direct numerical simulation of turbulent flow over a backward-facing step." *Journal of Fluid Mechanics*, Vol. 330, p. 349-374.

Lilly, D. K., 1992. "A proposed modification of the Germano subgrid-scale method." *Physics of Fluids A*, Vol. 4, p. 633-635.

Menter, F. R., 1994. "Two-Equation Eddy-Viscosity Turbulence Models for Engineering Applications." *AIAA Journal*, Vol. 32, No 8, p. 1598-1605.

Menter, F. R., Egorov, Y., 2010. "The Scale-Adaptive Simulation Method for Unsteady Turbulent Flow Predictions. Part 1: Theory and Model Description." *Flow Turbulence and Combustion*, v. 85, n. 1, p. 113-138.

Michelassi, V., Wissink, J. G., Rodi, W., 2003. "Direct numerical simulation, large eddy simulation and unsteady Reynolds-averaged Navier-Stokes simulations of periodic unsteady flow in a low-pressure turbine cascade: a comparison." In *Proceedings of the Institution of Mechanical Engineers Part a-Journal of Power and Energy*, v. 217, n. A4, p. 403-411, 2003.

Wilcox, D. C., 1986. "Multiscale model for turbulent flows." In *AIAA 24th Aerospace Science Meeting*. Reno, Nevada.

8. RESPONSIBILITY NOTICE

The authors are the only responsible for the printed material included in this paper.